

Meson Effects on Chiral Condensate at Finite Density

Mei Huang^{1,2}, Pengfei Zhuang¹, Weiqin Chao^{2,3}

¹ Physics Department, Tsinghua University, Beijing 100084, China

² CCAST, Beijing 100080, China

³ IHEP, Chinese Academy of Sciences, Beijing 100039, China

February 1, 2008

Abstract

Meson corrections on chiral condensate up to next-to-leading order in $1/N_c$ expansion at finite density are investigated in NJL model with chiral symmetry explicitly breaking. Compared with the mean-field results, the chiral phase transition is still of first order, while the properties at the critical density of chiral phase transition are found to change significantly.

PACS: 11.30.Rd, 11.10.Wx, 12.38.Lg

1 Introduction

It is generally believed that QCD undergoes chiral restoration at high temperature and density. The chiral condensate $\langle \bar{q}q \rangle$, which is regarded as the chiral order parameter, behaves quite differently as a function of baryon density ρ as compared to its variation with temperature T . At baryon density $\rho = 0$, quark condensate $\langle \bar{q}q \rangle$ does not change explicitly till $T \simeq 0.9T_c$, where T_c is the critical temperature. However, a model independent study [1] shows that the quark condensate decreases linearly with ρ at low density. At normal nuclear matter density, $\rho = \rho_0 = 0.17 fm^{-3}$, $\langle \bar{q}q \rangle$ has already decreased to about 2/3 of its vacuum value.

During the last decade, NJL model has been widely used to investigate chiral phase transition at finite temperature and density. Most publications were based on mean-field approximation, i.e., quark self-energy in the leading order of $1/N_c$ expansion and meson in random-phase approximation (RPA). At this level, the excited meson modes have no back interaction on quark self-energy. A thermal system described by NJL model in the mean-field approximation behaves as an effective free fermion gas, i.e., only quarks contribute to the thermal dynamical potential, while mesons do not play any role. This is clearly unphysical, since at least pion should play the dominant role at low temperature and density [2].

Therefore, it is necessary to go beyond the mean-field approximation, i.e., considering meson corrections to quark self-energy. In [3] and [4], the meson effects on chiral condensate at finite temperature have been investigated. Our work in this paper based on the self-consistent scheme of [5] [6] is to investigate the meson corrections on the chiral phase transition at finite density with $T = 0$.

2 Meson Corrections at $T = 0$ and $\mu = 0$

The two-flavor NJL model is defined through the Lagrangian density,

$$\mathcal{L} = \bar{\psi}(i\gamma^\mu\partial_\mu - m_0)\psi + G[(\bar{\psi}\psi)^2 + (\bar{\psi}i\gamma_5\vec{\tau}\psi)^2], \quad (1)$$

here G is the effective coupling constant of dimension GeV^{-2} , and m_0 is the current quark mass, assuming isospin degeneracy of the u and d quarks, and $\psi, \bar{\psi}$ are quark fields with flavor, color and spinor indices suppressed.

It is not easy to give the full expressions of quark self-energy and meson polarization functions self-consistently. Usually an approximation scheme called large N_c expansion is adopted. V. Dmitrašinović et al. proved in [5] that quark self-energy Σ and meson's polarization function Π_M shown in Fig. 1 are self-consistent to the subleading order in $1/N_c$ expansion and can keep all the chiral relations in the chiral limit. It is clear that the back interaction which conserves all the chiral properties is reflected in the contributions from the meson propagator to the quark mass, namely in $\delta\Sigma$.

Including current quark mass m_0 , the gap equation for quark mass can be expressed as

$$m = m_0 + \Sigma_H + \delta\Sigma, \quad (2)$$

where Σ_H and $\delta\Sigma$ are the leading and subleading order of quark self-energy in $1/N_c$ expansion, which can be read directly from the Feynman diagrams,

$$\Sigma_H = 8iGN_c N_f m \int \frac{d^4 p}{(2\pi)^4} \frac{1}{p^2 - m^2}, \quad (3)$$

$$\begin{aligned} \delta\Sigma = & -8GN_c N_f m \int \frac{d^4 p d^4 q}{(2\pi)^8} \left[\frac{(g_{\pi qq}^{(RPA)})^2}{q^2 - m_\pi^2} \left(\frac{3}{(p^2 - m^2)^2} \right. \right. \\ & - \left. \frac{3q^2}{(p^2 - m^2)^2((p+q)^2 - m^2)} \right) + \frac{(g_{\sigma qq}^{(RPA)})^2}{q^2 - m_\sigma^2} \left(\frac{1}{(p^2 - m^2)^2} \right. \\ & + \left. \frac{2}{(p^2 - m^2)((p+q)^2 - m^2)} - \frac{q^2 - 4m^2}{(p^2 - m^2)^2((p+q)^2 - m^2)} \right) \Big], \quad (4) \end{aligned}$$

where $g_{\pi qq}^{(RPA)}$ and $g_{\sigma qq}^{(RPA)}$ are meson coupling constant in RPA. At this position, it is necessary to point out that to keep the diagrams of meson corrections to quark self-energy and to meson polarization functions in the next-to-leading order in $1/N_c$ expansion properly, we have chosen the internal meson propagators in pole approximation.

Evaluating one quark loop integral, one can get a simple relation between the quark condensate and constituent quark mass m [5],

$$- \langle \bar{q}q \rangle = \frac{m - m_0}{4G}. \quad (5)$$

Meson polarization function Π_M ($M = \pi, \sigma$) can be written as

$$\Pi_M = \Pi_M^{(RPA)} + \delta\Pi_M, \quad (6)$$

where $\Pi_M^{(RPA)}$ and $\delta\Pi_M$ are pion polarization functions in the leading and subleading order of $1/N_c$ expansion, respectively, and

$$\delta\Pi_M = \delta\Pi_M^{(b)} + \delta\Pi_M^{(c)} + \delta\Pi_M^{(d)}. \quad (7)$$

Using the standard way of calculating Feynman diagrams, it is easy to write down the RPA polarization functions,

$$\begin{aligned} \Pi_M^{(RPA)} = & 4iN_cN_f \int \frac{d^4p}{(2\pi)^4} \frac{1}{p^2 - m^2} \\ & - 2iN_cN_f(k^2 - \epsilon_M 4m^2) \int \frac{d^4p}{(2\pi)^4} \frac{1}{(p^2 - m^2)((p+k)^2 - m^2)} \end{aligned} \quad (8)$$

with $\epsilon_\pi = 0$ and $\epsilon_\sigma = 1$.

After calculating the trace of quark loops, the meson corrections to the pion polarization function Π_π , corresponding to the three Feynman diagrams in Fig.1 can be expressed as:

$$\begin{aligned} \delta\Pi_\pi^{(b)}(k) = & 2N_cN_f \sum_{M=\pi,\sigma} \int \frac{d^4q d^4p}{(2\pi)^8} \frac{(g_{Mqq}^{(RPA)})^2}{q^2 - m_M^2} \\ & \left[\frac{1}{(p^2 - m^2)((p+q-k)^2 - m^2)} + \frac{1}{((p+q)^2 - m^2)((p-k)^2 - m^2)} \right. \\ & \left. - \frac{k^2(q^2 - \epsilon_M 4m^2)}{(p^2 - m^2)((p+q)^2 - m^2)((p-k)^2 - m^2)((p+q-k)^2 - m^2)} \right], \quad (9) \\ \delta\Pi_\pi^{(c)}(k) = & -4N_cN_f \sum_{M=\pi,\sigma} \int \frac{d^4q d^4p}{(2\pi)^8} \lambda_M \frac{(g_{Mqq}^{(RPA)})^2}{q^2 - m_M^2} \\ & \left[\frac{1}{((p+q)^2 - m^2)((p-k)^2 - m^2)} + \frac{k^2(q^2 - \epsilon_M 4m^2)}{(p^2 - m^2)^2((p+q)^2 - m^2)((p-k)^2 - m^2)} \right. \\ & + \frac{1}{(p^2 - m^2)^2} + \frac{2k \cdot q}{(p^2 - m^2)((p+q)^2 - m^2)((p-k)^2 - m^2)} \\ & \left. - \frac{k^2}{(p^2 - m^2)^2((p-k)^2 - m^2)} - \frac{(q^2 - \epsilon_M 4m^2)}{(p^2 - m^2)^2((p+q)^2 - m^2)} \right], \quad (10) \end{aligned}$$

with the degeneracy $\lambda_\pi = 3$, $\lambda_\sigma = 1$ and

$$\delta\Pi_\pi^{(d)}(k) = i \int \frac{d^4q}{(2\pi)^4} \frac{(g_{\pi qq}^{(RPA)})^2}{q^2 - m_\pi^2} \frac{(g_{\sigma qq}^{(RPA)})^2}{(q-k)^2 - m_\sigma^2} \left[\int \frac{d^4p}{(2\pi)^4} \frac{8mN_cN_f(k \cdot q - (p^2 - m^2))}{(p^2 - m^2)((p+q)^2 - m^2)((p+k)^2 - m^2)} \right]^2. \quad (11)$$

In the similar way, we can get the meson corrections to the sigma polarization functions. However, it should be careful that the upper meson propagator for $\delta\Pi_\pi^{(d)}$ in Fig. 1 can only be π , but for $\delta\Pi_\sigma^{(d)}$ it can be π and σ .

With the above quark self-energy and meson polarization functions, the meson mass m_M is determined through pole condition

$$1 - 2G\Pi_M(k^2 = m_M^2) = 0, \quad (12)$$

and the coupling constant g_{Mqq} is given by the residue at the pole

$$g_{Mqq}^{-2} = \partial\Pi_M/\partial k^2|_{k^2=m_M^2}. \quad (13)$$

Another important quantity is the pion decay constant f_π which is calculated from the vacuum to one-pion axial-vector matrix element. Replacing one vertex $i\gamma_5\vec{\tau}$ in Π_π by $ig_{\pi qq}\gamma_5\gamma_\mu\vec{\tau}/2$, we can get the simple relation

$$\frac{m_\pi^2 f_\pi}{g_{\pi qq}} = \frac{m_0}{2G}. \quad (14)$$

In the chiral limit, f_π satisfies the Goldberger-Treiman relation $f_\pi g_{\pi qq} = m$ [5].

3 Meson corrections at finite temperature and density

We now extend the above formulae of SU(2) NJL model beyond mean-field approximation to finite temperature and density in the frame of imaginary time temperature field theory.

At finite temperature using the Matsubara formalism and associated finite temperature Feynman rules, one arrives at the same integrals shown in the

last section with the replacement

$$\int \frac{d^4 p}{(2\pi)^4} \rightarrow \frac{i}{\beta} \sum_n \int_0^{\Lambda_F} \frac{d^3 \vec{p}}{(2\pi)^3} \quad (15)$$

for quark integration, with the zero-component of momentum p_0 replaced by $i\omega_n + \mu = (2n + 1)\pi T + \mu$, and

$$\int \frac{d^4 q}{(2\pi)^4} \rightarrow \frac{i}{\beta} \sum_n \int_0^{\Lambda_M} \frac{d^3 \vec{q}}{(2\pi)^3} \quad (16)$$

for internal meson integration, with the zero-component of momentum q_0 replaced by $i\nu_n = 2n\pi T$. Here T is temperature, μ the chemical potential, and the sums on n run over the Matsubara frequencies ω_n for quarks and ν_n for mesons.

While the $T = 0$ calculation could be performed using covariant, as well as non-covariant regularization prescriptions, at $T \neq 0$ Lorentz invariance is always broken and the physical $O(3)$ regularization restriction $|\vec{p}| < \Lambda$ presents itself most naturally. We take the pragmatic approach of applying this at finite temperature, and consider the device of the regularization scheme as part of the definition of the model. After the summation over the frequencies for quarks and internal mesons, one takes for external mesons the extension $i\alpha_l \rightarrow k_0 = m_M$.

Evaluation of frequency summation in two- and three-loop diagrams is not trivial, especially when two frequencies appear in a quark propagator or a meson propagator resulted from the energy conservation in Feynman rule.

4 Numerical results at finite density

As discussed in the beginning of this paper, the quark condensate behaves quite differently at finite density compared with that at finite temperature. The meson effects on chiral condensate at finite temperature has been investigated in [3] and [4]. In this paper, we focus our attention on the meson effects at finite density. The second reason to choose numerical study at finite density is technical: At $T = 0$ any frequency sum in imaginary time formulation is reduced to a step function of chemical potential which simplifies the momentum integration greatly.

As mentioned above, we introduced in our calculations the momentum cut-off Λ_F for quarks, Λ_M for pions and sigmas. We can not determine the four parameters for SU(2) NJL model, m_0 , G , and the three momentum cut-off Λ_F and Λ_M , since we know only two experimental observables $m_\pi = 139MeV$ and $f_\pi = 93.2MeV$ and an empirical value of quark condensate $\langle \bar{q}q \rangle = -(250 \pm 50MeV)^3$.

In [6], we have numerically investigated the NJL model parameters by fitting pion mass and pion decay constant with an appropriate current quark mass $m_0 = 5.5MeV$. The model parameters in the mean field approximation are $\Lambda_F = 637.7MeV$, $G\Lambda_F^2 = 2.16$, and $-\langle \bar{q}q \rangle^{1/3} = 248.0MeV$ with quark mass $m = 330MeV$. Going beyond mean-field approximation, we choose two series of NJL parameters: $\Lambda_F = 562.3MeV$, $G\Lambda_F^2 = 2.31$, and $-\langle \bar{q}q \rangle^{1/3} = 223.2MeV$ with $\Lambda_M/m = 1.5$ and $m = 330MeV$, and $\Lambda_F = 515.7MeV$, $G\Lambda_F^2 = 2.34$, $-\langle \bar{q}q \rangle^{1/3} = 218.2MeV$ with $\Lambda_M/m = 2$ and $m = 370MeV$. The degree of meson fluctuations is controled by the ratio Λ_M/m . It was found in [6], that for the first group parameters, the meson correction on chiral condensate is about 30% , and for the second group parameters, the meson correction is about 40%. The big correction in the second case arises from the big meson fluctuations characterized by the parameter Λ_M/m .

Our results of investigating chiral phase transition by using the above parameters will be shown as a function of the scaled density $n_b = \rho/\rho_0$, where $\rho_0 = 0.17fm^{-3}$ is the normal nuclear matter density, and $\rho = \frac{1}{3} \langle \psi^\dagger \psi \rangle = \frac{1}{3} \langle \bar{\psi} \gamma^0 \psi \rangle$ is the baryon density of the system, which has been calculated to the next-to-leading order in $1/N_c$ expansion. The scaled baryon density as a function of chemical potential μ is shown in Fig. 2, the stars correspond to the results in mean-field approximation, the pentagrams and the solid circles correspond to the results beyond mean-field approximation with the first and second group parameters, respectively.

The jumps in Fig. 2 show that chiral phase transition at finite density is of first order both in and beyond mean-field approximation. For the first group parameter, the lower critical density $n_b = 0.15$ is a little bit smaller than that in the mean-field approximation $n_b = 0.162$, and the upper critical density $n_b = 2.1$ is a little bit larger than the mean-field value $n_b = 1.93$. For the second group parameter, it is found that the lower critical density $n_b = 0.13$ is 20% smaller than the mean-field value, and the upper critical density $n_b = 2.79$ is 40% larger than that in mean-field approximation. In both cases, the meson corrections speed up the chiral phase transition, which

is similar to the results at zero density and finite temperature in [3], and extend the mixed phase of the first-order chiral transtion, while the degree of the change depends on the magnitude of the meson fluctuations.

We show the quark condensate scaled by its vacuum value $\langle \bar{q}q \rangle / \langle \bar{q}q \rangle_0$ in Fig. 3. *a*, as a function of the scaled density $n_b = \rho/\rho_0$. It is found that the quark condensate decreases to 30% of its vacuum value in the mean-field approximation, while it decreases to 10% of the vacuum value when meson corrections are included for the first group parameters, and even decreases to nearly zero for the second group parameters. This means that the meson corrections can help melt the chiral condensate more completely.

To show the meson effects at low density more clearly, we pick out the low density part of Fig. 3. *a* and enlarge it in Fig. 3. *b*. It is found that in the mean-field approximation, the chiral condensate and baryon density satisfy the linear relation [1]

$$\frac{\langle \bar{q}q \rangle}{\langle \bar{q}q \rangle_0} = 1 - \frac{\Sigma_{\pi N}}{f_\pi^2 m_\pi^2} \rho \quad (17)$$

before the phase transition, where the nucleon sigma term $\Sigma_{\pi N} = 0.043\text{GeV}$ is in good agreement with the experimental value 0.045GeV extrapolated from low energy pion-nucleon scatterings. However, when meson corrections are considered, this linear relation is more or less broken, depending on the degree of meson fluctutions.

5 Conclusions

In this paper we extended the self-consistent scheme of SU(2) NJL model beyond mean-field approximation and with chiral symmetry explicitly breaking to finite temperature and density, and calculated numerically the meson corrections to the quark condensate at finite density.

The numerical results show that the meson fluctuations can significantly change the properties of the system at finite density. Compared with the results in mean-field approximation, the meson fluctuations 1) speed up the chiral phase transition, 2) extend remarkbaly the mixed phase of the first-order chiral transition, 3) help melt the chiral condensate more completely, 4) break the linear relation between the quark condensate and the baryon density.

Acknowledgements

This work was supported in part by the NSFC under Grant No. 19925519 and the Major State Basic Research Development Program under Contract No. G2000077407.

References

- [1] W.Weise, Nucl. Phys. **A 610**(1996) 35c.
- [2] P.Zhuang, J.Hüfner, S.P.Klevansky, Nucl. Phys. **A 576**(1994)525.
- [3] W.Florkowski, and W.Broniowski, Phys.Lett.**B 386**(1996) 62.
- [4] P.Zhuang,Phys.Rev.**C 51**(1995) 2256.
- [5] V. Dmitrašinović, H-J. Schulze, R. Tegen and R. H. Lemmer, Ann.Phys. **238** (1995) 332.
- [6] M. Huang, P. F. Zhuang and W. Q. Chao, hep-ph/0102305.

The figure displays two rows of Feynman diagrams representing the decomposition of the quark self-energy Σ and the meson polarization function Π_M into their constituent parts.

Top Row: Quark Self-Energy (Σ)

- The first diagram is a shaded oval labeled Σ .
- An equals sign follows.
- The second diagram is a circle with a solid line and a dot at the bottom, labeled Σ_H .
- A plus sign follows.
- The third diagram is a circle with a solid line and a dot at the bottom, with a dashed loop on top labeled π, σ , labeled $\delta\Sigma$.

Bottom Row: Meson Polarization Function (Π_M)

- The first diagram is a shaded oval labeled Π_M .
- An equals sign follows.
- The second diagram is a circle with two solid lines and dots at the top and bottom, labeled $\Pi_M^{(RPA)}$.
- A plus sign follows.
- The third diagram is a circle with two solid lines and dots at the top and bottom, with a dashed loop on top labeled π, σ , labeled $\delta\Pi_M^{(b)}$.
- A plus sign follows.
- The fourth diagram is a circle with two solid lines and dots at the top and bottom, with a dashed loop on top labeled π, σ , labeled $\delta\Pi_M^{(c)}$.
- A plus sign follows.
- The fifth diagram is a circle with two solid lines and dots at the top and bottom, with a dashed loop on top labeled π, σ and a dashed loop on the bottom labeled σ , labeled $\delta\Pi_M^{(d)}$.

Figure 1: Quark self-energy Σ and meson polarization function Π_M in the quark and meson propagators. Σ_H and $\delta\Sigma$ are the leading and subleading contributions to the quark mass. $\Pi_M^{(RPA)}$ and $\delta\Pi_M^{(b,c,d)}$ are the leading and subleading order contributions to meson polarization function. The heavy solid lines indicate the constituent quark propagator, and the heavy dashed lines represent π or σ propagator $-iD_M^{(RPA)}(q)$ in RPA approximation.

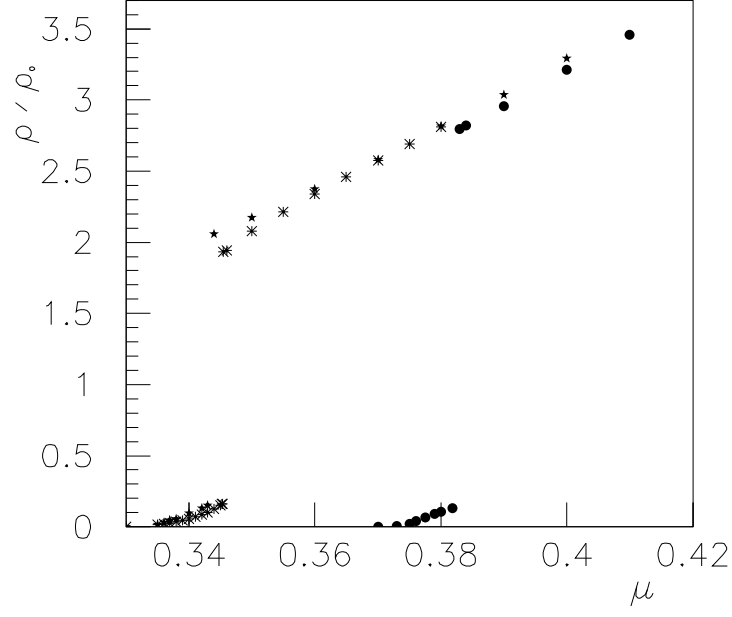


Figure 2: The scaled baryon density as a function of chemical potential μ , the stars correspond to the results in mean-field approximation, the pentagrams and the solid circles correspond to the results beyond mean-field approximation with the first and second group parameters, respectively.

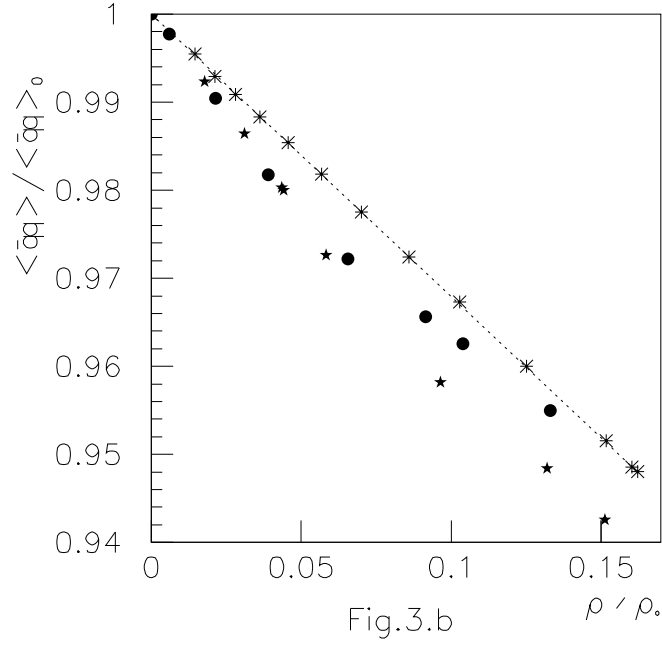
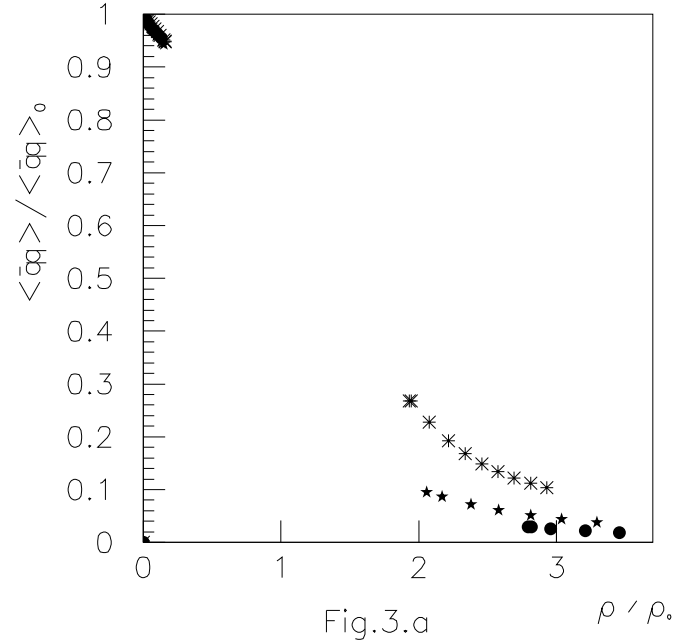


Figure 3: The scaled quark condensate in the whole density region (a) and only before the chiral phase transition (b) as a function of the scaled baryon density. The stars correspond to the results in mean-field approximation, and the pentagrams and the solid circles correspond to the results beyond mean-field approximation with the first and second group of parameters. The dashed line is used to represent the linear relation in mean-field case.